

# Crosstalk in Direct-Detection Optical Fiber FDMA Networks

Walid M. Hamdy and Pierre A. Humblet

Laboratory for Information and Decision Systems, M.I.T.,  
77 Massachusetts Avenue, Cambridge, MA 02139-4307.

## 1 Introduction

Direct-detection (DD) optical fiber frequency division multiple access (FDMA) is a simple and practical alternative to optical heterodyne FDMA. Previous works on estimating the performance of DD optical FDMA networks have usually focused only on the (linear) crosstalk degradation, typically relying on simplifying approximations such as the dominance of the adjacent channel interference [1], [4]. Other sources of performance degradation such as signal loss due to optical (predetection) and electrical (postdetection) filtering, intersymbol interference (ISI) due to the optical filtering, and channel beats (or nonlinear crosstalk) are usually ignored.

This paper presents a more precise analysis that takes into account the effect of optical and electrical filtering, ISI, and linear crosstalk [3]. The model used here is valid for arbitrary optical filter transfer functions and received pulse shapes. We consider in this paper only On-Off-Keyed (OOK) modulation; extending the analysis to Frequency-Shift-Keyed (FSK) modulation is straightforward, but is not discussed here.

## 2 System Model

The system is assumed to consist of  $M$  transmitter-receiver pairs connected by a star coupler. We assume for convenience that  $M$  is even. The received signal  $r(t)$  at each receiver is given by

$$r(t) = \sqrt{2} \sum_{i=-M/2}^{M/2-1} \sum_{k=-\infty}^{\infty} d_{ik} s(t - kT) \cos(2\pi f_i t + \phi_i) \quad (1)$$

where  $d_{ik} \in \{0, 1\}$  is the data bit transmitted by channel  $i$  during the  $k$ th bit period  $kT \leq t < (k+1)T$ ,  $f_i$  and  $\phi_i$  are the carrier frequency and phase of channel  $i$  respectively, and  $s(t)$  is the received pulse shape, normalized to unit energy. Note that all  $M$  channels are assumed to be bit-aligned. This results in a worst case linear crosstalk as shown in [2]. Laser phase noise and frequency chirp are ignored. We choose channel 0 (the center channel) to be the signal, with the other  $M-1$  channels being crosstalk. Strictly speaking, this is with some loss of generality since the filter frequency response is a weak function of the chosen channel. However, for most cases, this effect is small and can be neglected.

The front-end optical filter (see Fig. 1) is assumed throughout this paper to be linear time invariant (LTI) with an impulse response  $h(t)$  and with a system bandwidth of  $P$  Hz. For optical filters with an aperiodic frequency response,  $P$  equals the filter tuning range; for periodic optical filters  $P$  equals the frequency response period, or "free spectral range". The channel spacing  $\Delta f$  equals  $P/M$ . Shot noise is assumed negligible in comparison to the receiver thermal noise, as is usually the case in practical direct detection receivers. The photodetector thus acts as an ideal square-law detector with output current

$$i_d(t) = R_{pd} \left( \int_0^t h(\tau) r(t-\tau) d\tau \right)_{LP}^2 \quad (2)$$

where  $R_{pd}$  is the photodetector responsivity (henceforth set to 1). The subscript  $LP$  denotes removal of the double frequency terms.

The total receiver current is  $i(t) = i_d(t) + i_n(t)$ , where the noise current  $i_n(t)$  is assumed to be a zero mean AWGN process with double sided spectral density  $N_0/2$ . The current  $i(t)$  is subsequently low pass filtered (modeled

## Report Documentation Page

*Form Approved*  
*OMB No. 0704-0188*

Public reporting burden for the collection of information is estimated to average 1 hour per response, including the time for reviewing instructions, searching existing data sources, gathering and maintaining the data needed, and completing and reviewing the collection of information. Send comments regarding this burden estimate or any other aspect of this collection of information, including suggestions for reducing this burden, to Washington Headquarters Services, Directorate for Information Operations and Reports, 1215 Jefferson Davis Highway, Suite 1204, Arlington VA 22202-4302. Respondents should be aware that notwithstanding any other provision of law, no person shall be subject to a penalty for failing to comply with a collection of information if it does not display a currently valid OMB control number.

1. REPORT DATE <b>AUG 1991</b>	2. REPORT TYPE	3. DATES COVERED <b>00-08-1991 to 00-08-1991</b>		
4. TITLE AND SUBTITLE <b>Crosstalk in Direct-Detection Optical Fiber FDMA Networks</b>		5a. CONTRACT NUMBER		
		5b. GRANT NUMBER		
		5c. PROGRAM ELEMENT NUMBER		
6. AUTHOR(S)		5d. PROJECT NUMBER		
		5e. TASK NUMBER		
		5f. WORK UNIT NUMBER		
7. PERFORMING ORGANIZATION NAME(S) AND ADDRESS(ES) <b>Massachusetts Institute of Technology, 77 Massachusetts Avenue, Cambridge, MA, 02139-4307</b>		8. PERFORMING ORGANIZATION REPORT NUMBER		
9. SPONSORING/MONITORING AGENCY NAME(S) AND ADDRESS(ES)		10. SPONSOR/MONITOR'S ACRONYM(S)		
		11. SPONSOR/MONITOR'S REPORT NUMBER(S)		
12. DISTRIBUTION/AVAILABILITY STATEMENT <b>Approved for public release; distribution unlimited</b>				
13. SUPPLEMENTARY NOTES				
14. ABSTRACT				
15. SUBJECT TERMS				
16. SECURITY CLASSIFICATION OF:			17. LIMITATION OF ABSTRACT	
a. REPORT <b>unclassified</b>	b. ABSTRACT <b>unclassified</b>	c. THIS PAGE <b>unclassified</b>	18. NUMBER OF PAGES <b>11</b>	19a. NAME OF RESPONSIBLE PERSON

by an integrate and dump filter), sampled, and compared to a threshold. The sampled output for the 0th bit period is given by

$$\mathcal{E}(\mathbf{d}, M) = \int_0^T i_d(t)dt + \int_0^T i_n(t)dt = \mathcal{E}(\mathbf{d}, M) + \mathcal{N}. \quad (3)$$

The variable  $\mathcal{E}$  is the received energy, and is a function of the  $M$  data bits  $\mathbf{d} \triangleq \{d_i, i = -M/2, \dots, M/2 - 1\}$  sent by the  $M$  channels during  $[0, T]$ . The noise variable  $\mathcal{N}$  is a zero mean Gaussian random variable with variance  $\sigma^2 = N_0T/2$ . Assuming negligible ISI, we may approximate the received energy during each bit period by that collected with an infinite-time integrator

$$\mathcal{E}(\mathbf{d}, M) \approx \int_{-\infty}^{\infty} i_d(t)dt = \int_{-\infty}^{\infty} |H(f)|^2 |R(f)|^2 df. \quad (4)$$

This form simplifies the analysis considerably. Later, we shall correct for this approximation.

The energy  $\mathcal{E}(\mathbf{d}, M)$  is a sum of three components: a signal component  $\mathcal{S}(d_0, M)$ , a linear crosstalk component  $\mathcal{C}(\mathbf{d}^-, M)$ , and a nonlinear crosstalk, or channel beats, component  $\mathcal{B}(\mathbf{d}, M)$ . Here, by abuse of notation,  $\mathbf{d}^- \triangleq \mathbf{d} - d_0$ . The three components of  $\mathcal{E}$  can be written as

$$\mathcal{S}(d_0, M) = d_0 \int_{-\infty}^{\infty} |H(f)|^2 |S(f - f_0)|^2 df \quad (5)$$

$$\mathcal{C}(\mathbf{d}^-, M) \triangleq \sum_{\substack{i=-M/2 \\ i \neq 0}}^{M/2-1} d_i \int_{-\infty}^{\infty} |H(f)|^2 |S(f - f_i)|^2 df \quad (6)$$

$$\mathcal{B}(\mathbf{d}, M) \triangleq \sum_{\substack{i, l=-M/2 \\ l \neq i}}^{M/2-1} \frac{d_i d_l}{2} \int_{-\infty}^{\infty} |H(f)|^2 S(f - f_i) S^*(f - f_l) e^{-j(\phi_i - \phi_l)} + |H(f)|^2 S(f + f_i) S^*(f + f_l) e^{j(\phi_i - \phi_l)} df. \quad (7)$$

The sampled output is then

$$\mathcal{Z}(\mathbf{d}, M) = \mathcal{S}(d_0, M) + \mathcal{C}(\mathbf{d}^-, M) + \mathcal{B}(\mathbf{d}, M) + \mathcal{N} \quad (8)$$

i.e., the signal is corrupted by two non-Gaussian noises in addition to the Gaussian noise source. The expressions in (5)-(7) will enable us to determine the crosstalk degradation and signal energy reduction (due to the optical filter). This is done in the following Section. Later, we shall determine the additional losses caused by the electrical filtering (due to the finite time integration) and the ISI.

### 3 Analysis

Define

$$\mathcal{E}_i(d_i, M) \triangleq d_i \int_{-\infty}^{\infty} |H(f)|^2 |S(f - f_i)|^2 df \quad ; d_i \in \{0, 1\} \quad (9)$$

as the received energy from channel  $i$  when it sends  $d_i$ . Since the filter is centered on  $f_0$ , the carrier frequency of the signal, we may write (9) as

$$\mathcal{E}_i(d_i, M) = d_i \int_{-\infty}^{\infty} |H(\delta)|^2 |S(\delta - \frac{i}{M})|^2 d\delta \quad (10)$$

where  $\delta \triangleq f/P$  is normalized frequency. In particular, the signal energy equals

$$\mathcal{S}(d_0, M) = \mathcal{E}_0(d_0, M) = d_0 \int_{-\infty}^{\infty} |H(\delta)|^2 |S(\delta)|^2 d\delta. \quad (11)$$

Further simplification depends on whether  $|H(\delta)|^2$  is an periodic or aperiodic function. In the former case we may convert to the time domain to obtain

$$\mathcal{E}_i(d_i, M) = d_i \sum_{q=-\infty}^{\infty} \tilde{h}[q] \tilde{s}(q) e^{-j2\pi q i/M} \quad (12)$$

where  $\tilde{h}[q]$  are the Fourier coefficients of  $|H(\delta)|^2$  and  $\tilde{s}(n)$  are integer samples of the Fourier transforms of  $|S(\delta)|^2$ . In particular, the signal energy when a ONE is sent,  $\mathcal{S}(1, M)$ , equals

$$\mathcal{S}(1, M) = \sum_{q=-\infty}^{\infty} \tilde{h}[q]\tilde{s}(q). \quad (13)$$

Note that we assume an ideal extinction ratio, which gives  $\mathcal{E}_i(0, M) = 0$ .<sup>1</sup> The received energy is thus maximized when all  $M$  channels send ONE:

$$\begin{aligned} \mathcal{E}_{max}(M) &= \sum_{i=-M/2}^{M/2-1} \sum_{q=-\infty}^{\infty} \tilde{h}[q]\tilde{s}(q)e^{-j2\pi qi/M} \\ &= M \sum_{q=-\infty}^{\infty} \tilde{h}[qM]\tilde{s}(qM). \end{aligned} \quad (14)$$

From (13) and (14), the maximum crosstalk energy equals

$$\mathcal{C}_{max}(M) = \mathcal{E}_{max}(M) - \mathcal{S}(1, M) = M \sum_{q=-\infty}^{\infty} \tilde{h}[qM]\tilde{s}(qM) - \sum_{q=-\infty}^{\infty} \tilde{h}[q]\tilde{s}(q). \quad (15)$$

Similar expressions are obtained for optical filters with an *aperiodic* transfer function. A summary of these expressions are given in Table 1.

From (12) above we may also obtain the received energy probability mass function (pmf), which is given by the convolution of the  $M$  independent random variables

$$\mathcal{E}_i(d_i, M) = \begin{cases} 0 & ; d_i = 0 \text{ prob} = 1/2 \\ \mathcal{E}_i(1, M) & ; d_i = 1 \text{ prob} = 1/2, \end{cases} \quad (16)$$

where  $-M/2 \leq i \leq M/2 - 1$ , giving

$$p_{\mathcal{E}}(\mathcal{E}) = \bigotimes_{i=-M/2}^{M/2-1} \left[ \frac{1}{2}\delta(\mathcal{E}) + \frac{1}{2}\delta(\mathcal{E} - \mathcal{E}_i(1, M)) \right], \quad (17)$$

where  $\bigotimes$  denotes convolution and  $\delta(\cdot)$  is the Dirac delta function. The *crosstalk* pmf, denoted as  $\mathcal{C}(\mathbf{d}^-, M)$ , is obtained by removing the  $i = 0$  term in (17).

### 3.1 Filtering Penalty, Crosstalk Penalty and BER Computation

Ideally, the (normalized) received signal energy when a ONE is sent is 1. Filtering the signal energy reduces the signal energy to  $\mathcal{S}(1, M)$ . Therefore, the signal filtering penalty equals

$$X_{fit} \triangleq 10 \log_{10} \frac{1}{\mathcal{S}(1, M)}. \quad (18)$$

Similarly, the crosstalk penalty is the ratio of the signal distance with worst-case crosstalk to that without crosstalk. The former is equal to  $\mathcal{S}(1, M) - \mathcal{C}_{max}(M)$ , while the latter is  $\mathcal{S}(1, M)$ . The crosstalk penalty is thus

$$X_{cr} \triangleq 10 \log_{10} \frac{\mathcal{S}(1, M)}{\mathcal{S}(1, M) - \mathcal{C}_{max}(M)}. \quad (19)$$

To determine the bit error rate (BER) degradation, we first determine the expected energy output *conditional* on the data sent by the crosstalk channels

$$\begin{aligned} E(\mathcal{Z}|d_0 = 0, \mathbf{d}^-) &= \mathcal{C}(\mathbf{d}^-, M) \\ E(\mathcal{Z}|d_0 = 1, \mathbf{d}^-) &= \mathcal{S}(1, M) + \mathcal{C}(\mathbf{d}^-, M) \end{aligned}$$

<sup>1</sup>Extending the analysis to include non-zero extinction ratios is simple, but not considered here.

where  $\mathbf{d}^-$  is defined in Section 2. The noise variance is equal to  $\sigma^2 = N_0T/2$  for both ONE and ZERO. Thus, *conditional on* knowledge of the crosstalk pmf  $\mathcal{C}(\mathbf{d}^-, M)$ , our problem becomes the known problem of detecting binary signals in AWGN, with the threshold  $\gamma$  equal to  $(\mathcal{S}(1, M) + \mathcal{C}_{max}(\mathbf{d}^-, M))/2$ . This gives a probability of error

$$P_e = \frac{1}{2}E \left\{ Q \left( \frac{\gamma - \mathcal{C}(\mathbf{d}^-, M)}{\sigma} \right) + Q \left( \frac{\mathcal{S}(1, M) + \mathcal{C}(\mathbf{d}^-, M) - \gamma}{\sigma} \right) \right\} \quad (20)$$

where the averaging is performed over the crosstalk pmf  $\mathcal{C}(\mathbf{d}^-, M)$  and  $Q(x) \triangleq \int_x^\infty \frac{1}{\sqrt{2\pi}} e^{-x^2/2} dx$ .

## 4 Performance of FP filters

### 4.1 Frequency and Time Responses

An FP filter with mirror (power) reflectivity  $R$  has a (field) impulse response  $h(t)$  given by

$$h(t) = (1 - R) \sum_{i=0}^{\infty} R^i \delta(t - i/P) \quad (21)$$

and intensity frequency response

$$|H(f)|^2 = \frac{1 - R}{1 + R} \sum_{n=-\infty}^{\infty} R^{|n|} e^{-j \frac{2\pi n f}{F}}. \quad (22)$$

The Fourier coefficients of  $|H(f)|^2$  are thus

$$\tilde{h}[n] = \frac{1 - R}{1 + R} R^{|n|} \quad -\infty < n < \infty. \quad (23)$$

Alternatively, the squared frequency response is given by the Airy function

$$|H(f)|^2 = \frac{1}{1 + (2F/\pi)^2 \sin^2(\frac{\pi f}{F})} \quad (24)$$

where the Finesse  $F \triangleq \pi\sqrt{R}/(1 - R)$  and the Free Spectral Range (or period)  $P = c/2nL$ , with  $n$  the refractive index inside the cavity. The FP filter's full width at half maximum (FWHM)  $B$  equals  $B = P/F$ .

Fig. 2 shows the pulse response of an FP filter to a pulse with  $F = 100$  and  $1/BT = 0.5$  at resonance ( $\delta = 0$ ) and slightly off resonance ( $\delta = 0.03$ ). Notice the "relaxation resonance" in the off-resonance pulse response.

We find it convenient here to define the ratios

$$\alpha \triangleq 1/BT = \text{data rate / filter FWHM}$$

$$\beta \triangleq 1/T\Delta f = \text{data rate / channel spacing.}$$

Note that  $\alpha$  is filter dependent, while  $\beta$  is filter independent. For the FP filter  $\alpha = F/TP$  while  $\beta = M/TP$ , giving  $\beta/\alpha = M/F$  (= filter FWHM to channel spacing ratio).

### 4.2 Penalty Calculations

For a received NRZ pulse shape,  $s(t) = 1/\sqrt{T}$  for  $t \in [0, T]$  and zero elsewhere. It follows that

$$|S(\delta)|^2 = TP \left( \frac{\sin(\pi TP\delta)}{\pi TP\delta} \right)^2 \quad (25)$$

whose transform equals

$$\tilde{s}(\tau) = \begin{cases} 1 - \frac{|\tau|}{TP} & \tau \leq TP \\ 0 & \tau > TP. \end{cases} \quad (26)$$

Substituting (23) and (26) in (12) and (14), and assuming  $F \gg 1$  and  $\beta < 1$  we obtain

$$\mathcal{S}(1, M) \approx 1 - \frac{\alpha\pi}{4F^2} \operatorname{cosech}^2(\pi/2F) \approx 1 - \alpha/\pi \quad (27)$$

$$\begin{aligned}\mathcal{E}_{max}(M) &\approx \frac{\pi M}{2F} \left[ \coth(\pi M/2F) - \frac{M\alpha}{2F} \operatorname{cosech}^2(\pi M/2F) \right] \\ &\approx 1 - \frac{\alpha}{\pi} + \frac{\pi^2}{12} \left( \frac{M}{F} \right)^2 \left( 1 + \frac{\alpha}{\pi} \right)\end{aligned}\quad (28)$$

where we used the approximations  $\coth(x) \approx 1/x + x/3$  and  $\operatorname{cosech}(x) \approx 1/x - x/6$ , which are valid for small  $x$ . It follows from above that the worst-case crosstalk is given by

$$C_{max}(M) = \mathcal{E}_{max}(M) - \mathcal{S}(1, M) \approx \frac{\pi^2}{12} \left( \frac{M}{F} \right)^2 \left( 1 + \frac{\alpha}{\pi} \right). \quad (29)$$

The above formulas agree precisely with our previous results in [2], where we assumed  $\alpha = 0$  (i.e., zero-bandwidth or tone-like channels). In that case the signal energy and the crosstalk are given by 1 and  $\frac{\pi^2}{12} \left( \frac{M}{F} \right)^2$  respectively. Fig. 3 shows the energy pmf when an FP filter is used with  $M/F = 0.8$ . The two distinct and identical masses represent the possible energy levels received when the signal sent ZERO or ONE. This figure also shows the effect of increasing  $\alpha$ , which is to be interpreted here as increasing the data rate. The left (ZERO) mass shifts to the right (increasing crosstalk energy), while the right (ONE) mass shifts to the left (increasing the signal energy loss). Both effects result in a closing of the eye-opening (equivalently, a reduction in signal distance).

By substituting (27) in (18) we obtain the signal filtering penalty

$$X_{fil} = 10 \log_{10} \left( \frac{1}{1 - \frac{\alpha}{\pi}} \right) \quad (30)$$

which is shown in Fig. 4 (bottom solid line) as a function of  $\alpha$ . However, as mentioned earlier in Section 2, not all the filtered signal energy is collected by the integrate and dump filter since the integration is only over a finite period of length  $T$  and not over all time. This loss is referred to here as the finite time integration penalty. For general low pass filters, it is the electronic filtering penalty. In the case of the FP filter, optimizing the integration period (of duration  $T$ ) of a received pulse yields the signal energy  $1 - \frac{\ln 2 + 1/2}{\pi} \alpha$ , which is slightly less than  $1 - \alpha/\pi$ . Thus, the finite time integration penalty is

$$X_{fin} = 10 \log_{10} \left( \frac{1 - \frac{\alpha}{\pi}}{1 - (\ln 2 + 1/2) \frac{\alpha}{\pi}} \right). \quad (31)$$

The third signal related penalty is the ISI penalty which is a result of detecting energy from neighboring pulses in addition to the desired pulse. By considering only nearest neighbor pulses, we find that the ISI in turn reduces the signal distance from  $1 - (\ln 2 + 1/2) \frac{\alpha}{\pi}$  to  $1 - (2 \ln 2) \frac{\alpha}{\pi}$ , yielding an additional penalty equal to

$$X_{isi} = 10 \log_{10} \left( \frac{1 - (\ln 2 + 1/2) \frac{\alpha}{\pi}}{1 - (2 \ln 2) \frac{\alpha}{\pi}} \right). \quad (32)$$

Finally, we have the crosstalk penalty. Here we use the signal energy after both optical and electrical filtering as well as ISI as the baseline (or numerator of log argument), giving a crosstalk penalty equal to

$$X_{er} = 10 \log_{10} \left( \frac{1 - (2 \ln 2) \frac{\alpha}{\pi}}{1 - (2 \ln 2) \frac{\alpha}{\pi} - \frac{\pi^2}{12} (M/F)^2 (1 - \frac{\alpha}{\pi})} \right). \quad (33)$$

Fig. 4 is a plot of the cumulative penalty as a function of  $\alpha$ . The first three penalties above are signal-related, and thus are zero for  $\alpha = 0$ . The crosstalk penalty, however, is nonzero even for  $\alpha = 0$ , due to the  $M/F$  factor.

### 4.3 BER degradation

The BER degradation with increasing  $\alpha$  is obtained by (numerically) computing the crosstalk pdf  $\mathcal{C}(d^-, M)$ , and using it as shown in (20). An example is shown in Fig. 5 for  $M/F = 0.4$ . Here the signal to noise ratio (SNR) is defined as  $\text{SNR} \triangleq 1/\sigma$ , where  $\sigma = N_0 T/2$  is the noise variance. Thus the SNR is referred to the *input* of the optical filter.

## 5 Performance of Multistage MZ filters

### 5.1 Physical Structure and Power Transfer Function

An ideal single-stage Mach-Zehnder (MZ) filter consists of two ideal 3-dB couplers connected by two waveguides of length difference  $\Delta L$  (see Fig. 6(a)). The power transfer function of the two output ports referenced to the same input port are given by

$$|H_1(f)|^2 = \cos^2\left(\frac{\pi f}{P}\right) \quad |H_2(f)|^2 = \sin^2\left(\frac{\pi f}{P}\right) \quad (34)$$

where  $P = c/n\Delta L$  is the transfer function period.

To construct a multistage MZ filter, single-stage MZ filters are cascaded in a manner such that the length difference of stage  $i$  is double that of stage  $i - 1$ , with the first stage having a length difference  $\Delta L$  as in Fig. 6(b) (see also [5], [6]). The overall transfer function of a  $K$ -stage MZ filter is given by

$$|H(\delta)|^2 = \prod_{i=1}^K \cos^2(\pi 2^{i-1} \delta) = \frac{\sin^2(\pi M \delta)}{M^2 \sin^2(\pi \delta)}, \quad M = 2^K \quad (35)$$

with Fourier coefficients

$$\tilde{h}[n] = \begin{cases} \frac{M-|n|}{M^2} & |n| \leq M \\ 0 & \text{otherwise.} \end{cases} \quad (36)$$

Fig. 7 shows the transfer functions of three stages comprising a 3-stage MZ filter and Fig. 8 shows one-period of the resulting transfer function. By placing all but the signal channel in the  $2^{K-1}$  nulls of one period of the overall transfer function and the signal channel in the passband, the crosstalk may be strongly suppressed. However, the non-zero channel bandwidths as well as any filter imperfections naturally prevent a total crosstalk suppression. The filter FWHM  $B$  is narrowed as the number of stages increases, since for large  $K$  we may show that

$$B \approx \frac{2.8}{\pi} \frac{P}{2^K}. \quad (37)$$

The envelope of the transfer function is closely approximated by an Airy function (Eq. (24))

$$|H(\delta)|^2 \approx \frac{1}{1 + M^2 \sin^2(\pi \delta)},$$

where the Finesse  $F = \pi M/2$ . The accuracy of this approximation can be seen from Fig. 9. Note that this Airy function has a smaller FWHM than that of the MZ filter it approximates. Thus an FP filter with the above Finesse will produce both more crosstalk and more signal loss than the MZ filter. As a result, the performance of this FP filter is a *lower* bound on the MZ filter performance. For example, an ideal MZ filter with  $K = 7$  stages will perform no worse than an FP filter of finesse  $F \approx 200$ .

### 5.2 Temporal Responses

By construction, the  $i^{\text{th}}$  stage of a  $K$ -stage MZ filter has two paths of length difference  $\Delta L_i = 2^{i-1} \Delta L$ , where  $\Delta L$  is the length difference of the first, or “coarsest”, stage. In effect then, an input impulse “sees” exactly  $2^K$  different paths of lengths  $0, \Delta L, \dots, (2^K - 1)\Delta L$ . Thus a  $K$ -stage MZ filter is a finite impulse response (FIR) filter with an impulse response given by a finite train of impulses of spacing  $\Delta t = n\Delta L/c = 1/P$  and of equal height  $2^{-K} = 1/M$ .

In contrast to our analysis of the FP filter model, we shall find it more convenient to express our results in terms of  $\beta$  instead of  $\alpha$ . However, these two quantities are dependent variables here since, by using (37),

$$\beta \triangleq \frac{1}{T\Delta f} = \frac{B}{\Delta f} \frac{1}{BT} \approx \frac{2.8}{\pi} \alpha \quad \text{for large } M. \quad (38)$$

Fig. 10 shows the pulse response of a 7-stage MZ filter to two (unit intensity) pulses with  $\beta = 0.25$  and 2. As can be seen, for minimal pulse distortion  $\beta$  has to be smaller than 1, allowing the pulse response to be concentrated in a  $T$ -second long period, and to approach its ideal value of 1 during that period.

### 5.3 Penalty Calculations

Substituting (36) and (26) in (12), we obtain

$$\mathcal{E}_i(1, M) = \begin{cases} \frac{\beta}{M^2 \sin^2(\pi i/M)} & i \neq 0 \\ 1 - \frac{\beta}{3} \left( \frac{M^2 - 1}{M^2} \right) & i = 0 \end{cases} \quad (39)$$

and

$$\mathcal{E}_{max}(M) = 1. \quad (40)$$

The last equation is exact and is independent of  $\beta$ . It follows directly from (39) and (40) that

$$\mathcal{S}(1, M) \approx 1 - \beta/3 \quad \text{for large } M \quad (41)$$

and

$$\mathcal{C}_{max}(M) = \frac{\beta}{3} \left( \frac{M^2 - 1}{M^2} \right) \approx \beta/3 \quad \text{for large } M. \quad (42)$$

The filtering penalty is thus

$$X_{fil} = 10 \log_{10} \left( \frac{1}{1 - \beta/3} \right). \quad (43)$$

Finding the finite time integration penalty is done as with the FP filter; the integration period position is chosen to maximize the received energy. Some simple algebra reveals that the maximum received energy during a  $T$ -second is  $1 - 5\beta/12$ , thus giving a finite time integration penalty of

$$X_{fin} = 10 \log_{10} \left( \frac{1 - \beta/3}{1 - 5\beta/12} \right). \quad (44)$$

Similarly, the ISI penalty is found following the same procedures used with the FP filter to be

$$X_{isi} = 10 \log_{10} \left( \frac{1 - 5\beta/12}{1 - \beta/2} \right). \quad (45)$$

From above, the crosstalk penalty becomes independent of  $M$  for large  $M$ . Again, by measuring the penalty from the filtering+finite time integration+ ISI signal energy baseline, we get

$$X_{cr} = 10 \log_{10} \left( \frac{1 - \beta/2}{1 - 5\beta/6} \right). \quad (46)$$

Fig. 11 is a plot of the resulting cumulative penalty.

### 5.4 BER Degradation

Computing the BER degradation follows steps identical to those used in the FP filter example. The difference is in the values of  $\mathcal{S}(1, M)$  and  $\mathcal{C}(d^-, M)$ . Fig. 12 shows the BER degradation with  $\beta$  for  $K = 4$  stages.

## 6 Multistage MZ Filter Imperfections

In this Section we discuss two crucial imperfections unique to multistage MZ filters. These imperfections may cause the performance obtained with these filters to be seriously degraded, and are therefore worth considering.

### 6.1 Imperfect Coupling Ratios

An ideal multistage MZ filter is constructed with ideal 3 dB couplers. If the coupling ratio deviates from 50:50, then the filter response changes significantly. Let  $|\epsilon_{1i}|, |\epsilon_{2i}| \ll 1$  be the deviations of the coupling ratios of the first and second 3 dB coupler in the  $i$ th MZ stage. Using a first order series approximation, we find that the crosstalk penalty with  $\beta = 0$  is given by

$$10 \log_{10} \left( \frac{1 - 2 \sum_{i=1}^K \gamma_{1i} + \sum_{i=1}^K \gamma_{2i}}{1 - 2 \sum_{i=1}^K \gamma_{1i}} \right) \quad (47)$$



where  $\gamma_{1i} = \epsilon_{1i}^2 + \epsilon_{2i}^2$  and  $\gamma_{2i} = (\epsilon_{1i} - \epsilon_{2i})^2$ . The filtering plus crosstalk penalty, on the other hand, depends only on the  $\gamma_{1i}$  and equals

$$10 \log_{10} \left( \frac{1}{1 - 2 \sum_{i=1}^K \gamma_{1i}} \right). \quad (48)$$

This penalty is shown for several values of  $K\gamma$  in Fig. 13, where we have assumed for simplicity that  $\gamma_{1i} = \gamma$ .

## 6.2 Stage Misalignment

Another possible imperfection in MZ filters is an error in the misalignment of the stages such that the resonances do not coincide as in Fig. 7. Using a second-order series approximation and after considerable algebra, we find that the filtering plus crosstalk penalty may be expressed as

$$10 \log_{10} \left( \frac{1}{1 - 2\pi^2 \sum_{i=1}^K \epsilon_i^2} \right) \quad (49)$$

where  $\epsilon_i$  is the normalized deviation of stage  $i$  from its ideal length, the normalization factor being the signal wavelength  $\lambda_0 = c/f_0$ . Fig. 14 shows the increase in crosstalk energy due to stage asynchronism for several values of  $K$  and the sensitivity increase with the number of stages.

## 7 Summary and Conclusions

We have presented an analysis of the performance of direct detection optical fiber FDMA networks in the presence of linear crosstalk, optical and electrical filtering, and signal ISI. We used the developed model and theory to analyze the performance of FP filters and multistage MZ filters as channel demultiplexers. Our results show that the degradations due to signal filtering and linear crosstalk are roughly of equal magnitude for practical system operating points, with finite time integration and ISI effects being of less significance. However, filter imperfections such as filter loss (not discussed here), nonideal coupling ratios, and stage misalignment may significantly reduce the obtainable performance. The additional effect of channel beats is complicated by the need to assume channel bit-*asynchronism* and will be considered in future research.

## 8 Acknowledgments

This research was supported by DARPA under grant F19628-90-C-0002 and by the U.S. Army Research Office under contract DAAL03-86-K-0171 (Center for Intelligent Control Systems).

## 9 References

- [1] I. P. Kaminow, P. P. Iannone, J. Stone and L. W. Stulz, "FDMA-FSK Star network with a tunable optical filter demultiplexer", *J. Lightwave Technol.*, Vol. 6, pp. 1406-1414, 1988.
- [2] P. A. Humblet and W. M. Hamdy, "Crosstalk Analysis and Filter Optimization of Single- and Double-Stage Fabry-Perot Filters", *J. on Sel. Areas in Comm.*, Vol. 9, pp. 1095-1107, 1990.
- [3] W. M. Hamdy, *Crosstalk in Direct Detection Optical FDMA Networks*, Ph.D Thesis, Massachusetts Institute of Technology, September 1991.
- [4] A. A. M. Saleh and J. Stone, "Two-stage Fabry-Perot filters as demultiplexers in optical FDMA LAN's", *J. Lightwave Technol.*, Vol. 7, pp. 323-330, 1989.
- [5] H. Toba *et. al.*, "Factors Affecting the Design of Optical FDM Information Distribution Systems", *J. on Sel. Areas in Comm.*, Vol. 9, pp. 948-964, 1990.
- [6] H. Toba, K. Inoue, and K. Nosu, "A conceptual design on optical frequency-division-multiplexing distribution systems with optical tunable filters", *IEEE J. on Sel. Areas in Comm.*, Vol. 4, pp. 1458-1467, 1986.

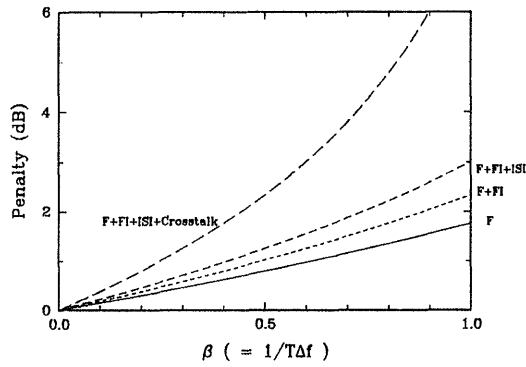


Figure 11: A plot of the various penalties with an MZ filter as a function of  $\beta$  for large  $K$ . Notation: F: filtering. F+FI: filtering + finite time integration. F+FI+ISI: filtering + finite time integration + ISI.

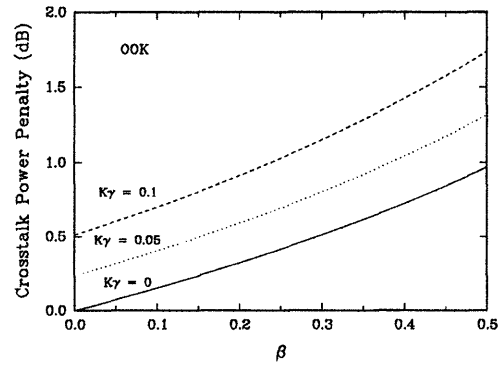


Figure 13: Effect of splitting ratio mismatch on the crosstalk penalty of a 6-stage MZ filter with OOK. Here  $\gamma_{1i} = \gamma_{2i} = \gamma$ .

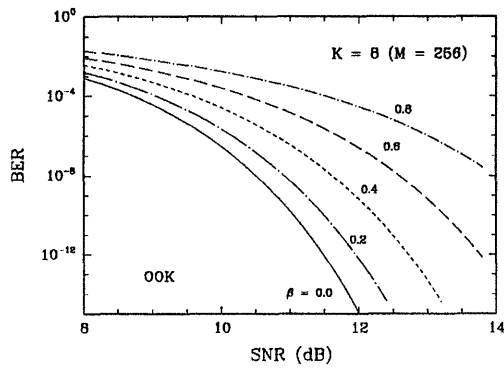


Figure 12: BER degradation with an 8-stage MZ filter and OOK.

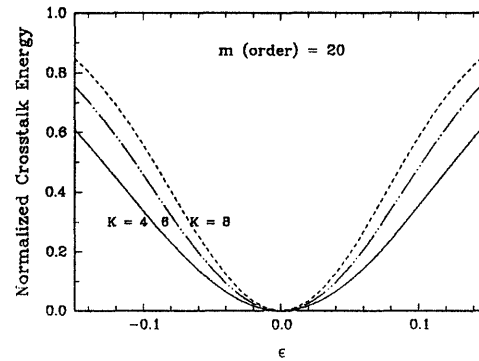


Figure 14: Increased crosstalk energy due to stage asynchronism as a function of  $\epsilon$ . Sensitivity increases with number of stages.  $m$  is the order of the resonance used for channel selection

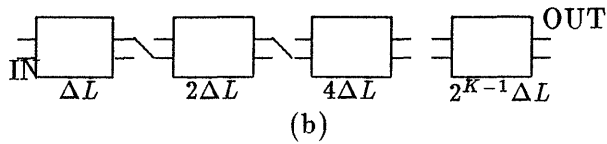
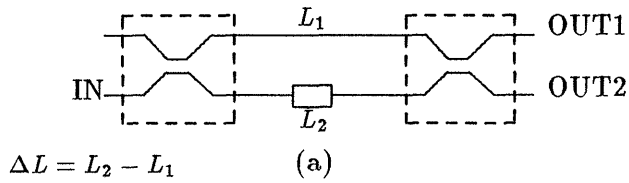


Figure 6: (a) Ideal single stage MZ filter with length differential  $\Delta L$  (b) Construction of a K-stage MZ filter. Each stage is marked with the appropriate length differential.

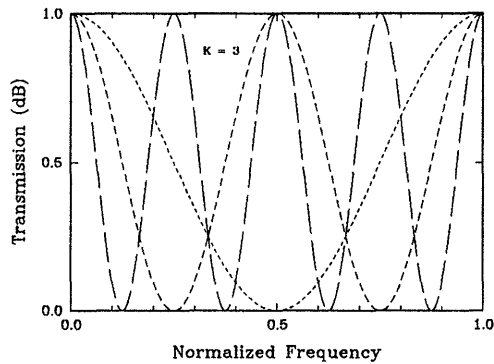


Figure 7: Frequency responses of each stage of a 3-stage MZ filter Overall transfer function of the 3-stage MZ filter.

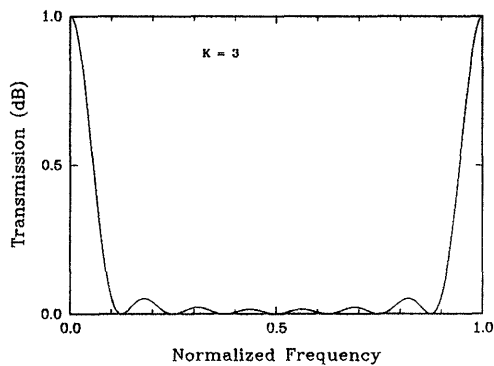


Figure 8: Overall transfer function of a 3-stage MZ filter.

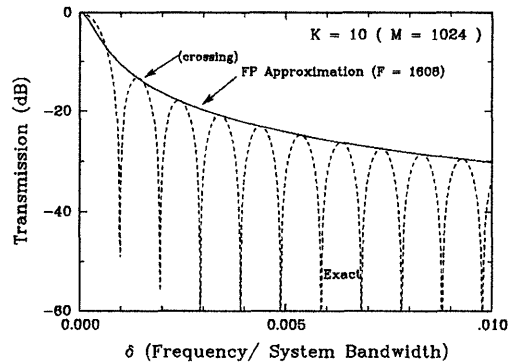


Figure 9: Approximating the upper envelope curve of an MZ frequency response with a frequency response of an "equivalent" FP filter. Case shown is for  $K = 10$  and  $F = 1608$ .

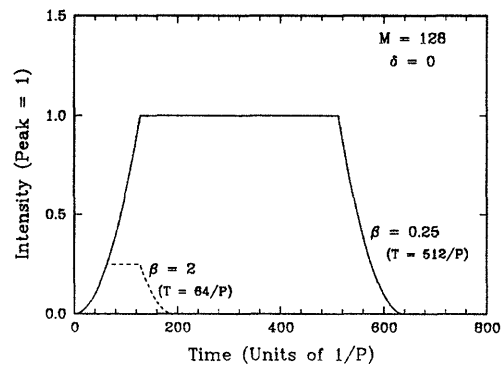


Figure 10: Pulse response of a 7-stage MZ filter with normalized input frequency  $\delta = 0$ . Shown in the figure are the response due to two pulse of duration  $\beta < 1$  and  $\beta > 1$ .

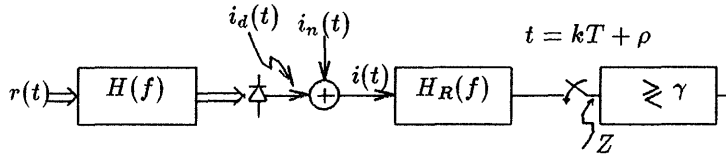


Figure 1: Receiver structure: Optical filter - Detector - Electric low pass filter.  $\rho (< T)$  is the time shift required to maximize the received signal energy.

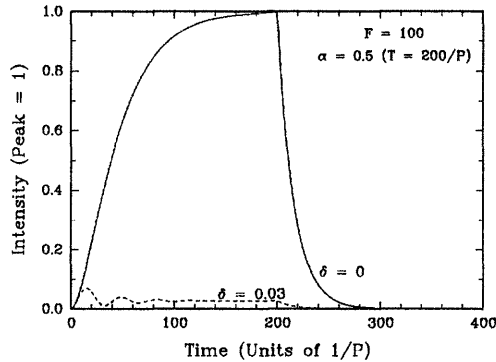


Figure 2: Pulse response of an FP filter with  $F = 100$  to a pulse of width  $T = 200/P$ .

Quantity	Aperiodic Filter	Periodic Filter
$\mathcal{E}_i(1, M)$	$\int_{-\infty}^{\infty} \tilde{h}(\tau) \tilde{s}(\tau) e^{-j2\pi\tau/M} d\tau$	$\sum_{q=-\infty}^{\infty} \tilde{h}[q] \tilde{s}(q) e^{-j2\pi qi/M}$
$S(1, M)$	$\int_{-\infty}^{\infty} \tilde{h}(\tau) \tilde{s}(\tau) d\tau$	$\sum_{q=-\infty}^{\infty} \tilde{h}[q] \tilde{s}(q)$
$\mathcal{E}_{max}(M)$	$\int_{-\infty}^{\infty} \tilde{h}(\tau) \tilde{s}(\tau) \frac{\sin(\pi\tau)}{\sin(\pi\tau/M)} e^{j\pi\tau/M} d\tau$	$M \sum_{q=-\infty}^{\infty} \tilde{h}[qM] \tilde{s}(qM)$

Table 1: Comparison of Aperiodic and Periodic Filter Output Energy Expressions

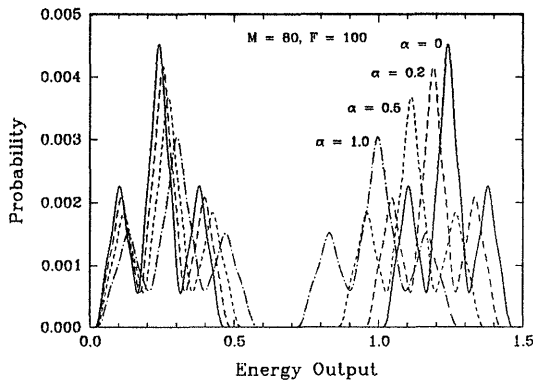


Figure 3: Energy pmf with FP filter.  $F=100, M=80$ .

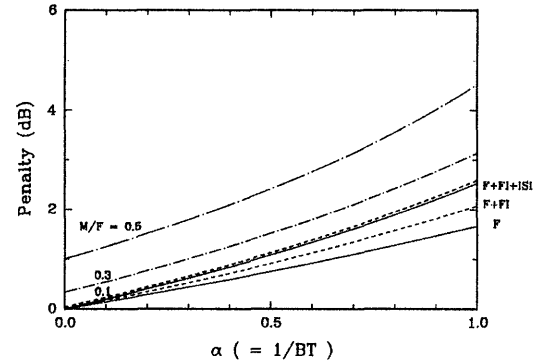


Figure 4: A plot of the various penalties for different  $M/F$  with an FP filter as a function of  $\alpha$ . Notation: F: filtering. F+FI: filtering + finite time integration. F+FI+ISI: filtering + finite time integration + ISI. Other curves include F+FI+ISI plus crosstalk at several values of  $M/F$ .

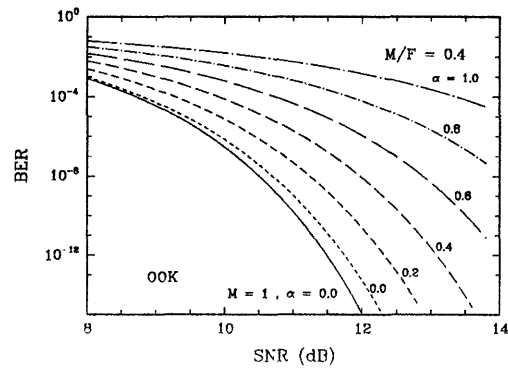


Figure 5: BER crosstalk induced degradation with an FP filter with  $M/F = 0.4$ . Also shown for comparison is the BER curve for one channel (no crosstalk).